Synchronized Dynamics of *Tipula paludosa* Metapopulation in a South-Western Scotland Agroecosystem: Linking Pattern to Process

Daniel Bearup, Sergei Petrovskii[1]

Department of Mathematics, University of Leicester,
University Road, Leicester LE1 7RH, U.K.
Emails: djb69@le.ac.uk, sp237@le.ac.uk

Rod Blackshaw

Centre for Agricultural and Rural Sustainability, University of Plymouth,
Drake Circus, Plymouth PL4 8AA, U.K.
Email: r.blackshaw@plymouth.ac.uk

Alan Hastings

Department of Environment Science and Policy, University of California at Davis,
Davis, CA 95616, USA.
Email: amhastings@ucdavis.edu

Keywords: metapopulation, synchronization, dispersal, Moran effect, *T. paludosa*

Publication type: article

Additional elements of the expanded online edition: Appendix

Figures to print in color: Figs. 1, 2 and 11

[1]Corresponding author. Phone/fax: +44 116 252 3916/3915, email: sp237@le.ac.uk

Abstract

Synchronization of population fluctuations at disjoint habitats has been observed in many studies but its mechanisms often remain obscure. Synchronization may appear as a result of either inter-habitat dispersal or because of regionally correlated environmental stochastic factors, the latter being known as the Moran effect. In this paper, we consider the population dynamics of a common agricultural pest insect *T. paludosa* on a fragmented habitat by analyzing data derived from a multi-annual survey of its abundance in 38 agricultural fields in South-West Scotland. We use cross-correlation coefficients and show that there is a considerable synchronization between different populations across the whole area. The correlation strength exhibits an intermittent behavior so that close populations can be virtually uncorrelated but populations separated by distances up to about 150 kilometers can have a cross-correlation coefficient close to one. In order to distinguish between the effects of stochasticity and dispersal, we then calculate a time-lagged cross-correlation coefficient and show that it possesses considerably different properties to the non-lagged one. In particular, the time-lagged correlation coefficient shows a clear directional dependence. The distribution of the time-lagged correlations with respect to the bearing between the populations has a striking similarity to the distribution of wind velocities, which we regard as evidence of long-distance wind-assisted dispersal.

1 Introduction

Understanding of population dynamics in complex environments has been one of the main challenges both for theoretical and empirical ecology over the last few decades (Levin 1976; Kareiva 1990; Lundberg et al. 2000). Environment is known to shape the geometry of ecological interactions through a variety of specific spatial and spatiotemporal mechanisms such as landscape structure (Pickett and Thompson 1978; Kaitala et al. 2001), seasonality and solar cycles (Sinclair and Gosline 1997), and transient weather conditions both on global and regional scale (Baars and Van Dijk 1984; Post and Forchhammer 2002; Raimondo et al. 2004). The latter is usually regarded as environmental stochasticity or noise; e.g. see Vasseur and Yodzis (2004) and references therein.

Landscape heterogeneity often results in a situation where populations of the same species occupy disjoint habitats. Depending on the inter-habitat distance, individual mobility and the nature of the environment between the habitats, e.g. how harsh it is, these local populations may or may not interact with each other through dispersal. The classic concept of metapopulation (Hanski and Gilpin 1991) refers to the case where the sizes of local populations fluctuate independently, thus assuming that the dispersal coupling between them can be neglected. In many cases, however, this is not the case and the population fluctuations in different habitats appear to be, to a certain extent, correlated (so that the metapopulation concept had to be updated accordingly, e.g. see Haydon and Steen 1997; Sutcliffe et al. 1997). This phenomenon is known as synchronization, and inter-habitat dispersal has been identified as a synchronizing factor (Liebhold et al. 2004). There is considerable evidence that dispersal coupling by just a tiny fraction of the population may bring population fluctuations into synchrony (Haydon and Steen 1997; Kendall et al. 2000; Ripa 2000).

Remarkably, dispersal coupling is not the only factor resulting in population synchronization. The impact of spatially correlated environmental noise on disconnected populations can synchronize the population fluctuations too, the phenomenon being known as the Moran effect (Moran 1953a,b; Royama 1992; Ranta et al. 1997). Having originally been discovered theoretically (cf. "Moran's theorem"), it has later been widely observed in different taxa and in various environments (Liebhold at al. 2004). Synchronization of population fluctuations can therefore be driven by the regional environmental stochasticity, by the interaction between local populations through dispersal, or by a mixture of both (Goldwyn and Hastings 2011). Without any impact from the Moran effect, dispersal

is typically too weak a force to produce synchrony (Goldwyn and Hastings 2011), but the Moran effect alone cannot produce very high levels of synchrony. What is less clear is the relative importance of these two forces.

Synchronization has many implications across the whole range of ecological sciences. Good understanding of patterns and mechanisms of synchronization is required in order to efficiently manage issues arising in agro-ecology (Rosenstock et al. 2011), in pest control (Milne et al. 1965; Blackshaw 1983; Williams and Liebhold 1995) and in nature conservation programs (Earn et al. 2000). Identifying particular factor(s) resulting in synchronization is therefore important. Indeed, linking an observed ecological pattern to a specific process has been a major issue in contemporary ecology (Levin 1992). However, since both dispersal and the Moran effect can have a similar impact on population dynamics, it is often very difficult to distinguish between them unless direct measures of the effect of dispersal are possible. For example, observed synchronies in the yield of pistachio trees must be due only to the Moran effect as there is no equivalent to dispersal in this system and this is confirmed by models (Lyles et al. 2009). But a system where dispersal can be eliminated as a force causing synchrony is rare, and differentiating the effects of stochasticity from that of dispersal is sometimes regarded as one of the greatest challenges to ecologists studying spatiotemporal population dynamics (Liebhold et al. 2004).

Another challenging problem is to identify the corresponding spatial scale of the mechanisms involved. For species with low mobility, the scale of synchronization due to dispersal is known to be smaller than the scale induced by the regional stochasticity. In particular, in a field study on butterflies, Sutcliffe et al. (1996) showed that the spatial scale of dispersal coupling is on the order of 5 kms while population synchrony can be observed on much larger distances of up to 200 kms. The larger spatial scale of synchronization is therefore likely to be linked to regional stochasticity, although this may not always be true if insect dispersal is assisted by the wind. Synchronization of population dynamics has been observed for many other insect species (Baars and Van Dijk 1984; Hanski and Woiwod 1993; Sutcliffe et al. 1996; Peltonen et al. 2002), although the specific factors responsible for synchronization were not always clear. Other striking examples of patterns of synchrony come from the dynamics of childhood diseases (Rohani et al. 1999). This study shows the importance of interactions between dispersal and dynamics since two diseases, measles and pertussis, show very different spatiotemporal patterns even though the dispersal parameters must be the same.

In this paper, we consider how the spatial pattern observed in population dynamics of an insect species dwelling on a habitat consisting of an array of agricultural fields can be affected by the landscape properties and by the weather conditions. The focus of this study is on *T. paludosa* which is a common pest in the British Islands and can cause significant damage to agriculture (Blackshaw and Coll, 1999). For this reason, its dynamics has been a focus of numerous field studies (Milne et al., 1965; Mayor and Davies, 1976; Blackshaw, 1983) as well as some theoretical work (Blackshaw and Petrovskii, 2007).

In order to address the issues of pattern, process and scale, we have analyzed annual data on the population abundance of *T. paludosa* collected between 1980 and 1994 in a few dozen agricultural fields across South-Western Scotland. Analysis of the time series of population density obtained at different locations across the region shows that the fluctuations in the abundance of *T. paludosa* are not independent. However, the synchronization pattern that we have observed exhibits some rather counter-intuitive properties. There is a considerable degree of synchronization between some of the fields but an absence of synchronization between others. Note that the generic dependence of synchronization on the inter-habitat distance is well known, with the degree of synchronization between different populations usually decreasing with distance (e.g. Sutcliffe et al. 1996; also Lundberg et al. 2000; Liebhold et al. 2004). However contrary to this, synchronization between *T. paludosa* abundances in different fields does not show any clear relation to the inter-field distance. Furthermore, we show that the observed synchronization pattern has a distinct directional aspect. In particular, while the north-west and south-east areas of the region are on average strongly correlated, there is much less correlation between the north-east and south-west areas. By linking this directional asymmetry to weather data, we show that it is likely to result from wind-assisted dispersal. In order to distinguish the effect of dispersal from that of stochasticity, we introduce a delay-based cross-correlation coefficient and show that it exhibits a pattern of directional dependence very similar to that of the wind velocity.

2 Methods

2.1 Species

Tipula paludosa Meig., the marsh cranefly, are found in cool temperate regions of northern Europe and the USA (Jackson and Campbell 1975). *T. paludosa* is univoltine with peak

adult emergence between mid-August and mid-September in the UK. Mature *T. paludosa* are flying insects and thus are found in a range of environments. However, dispersal is thought to be limited as females are poor fliers, emerging gravid and typically laying eggs within twelve hours of emergence (Blackshaw and Coll 1999). The larval stages of *T. paludosa*, known as leatherjackets, are soil dwelling and relatively lacking in mobility; consequently they are restricted to the locality in which they hatch. They feed primarily on the roots and stems of grasses and cereals, although they are also able to consume a variety of other crops (Blackshaw and Coll 1999). Leatherjackets are considered an agricultural pest, although it is relatively rare for them to destroy a sward. A substantial body of work postulates that leatherjacket populations can be affected by environmental conditions, specifically by the average rainfall prior to hatching. However, a significant effect (that may even result in a population crash) is only seen when weather conditions in September/October are exceptionally dry (Milne et al. 1965). On the other hand, temperature was shown to have little effect on *T. paludosa* dynamics (Blackshaw and Moore 2012). Correspondingly, other studies suggest that the environmental factors may be less significant than the effects of population density, especially in a harsh environment. In particular, contest competition through combat between leatherjackets is posited as the mechanism for this population regulation (Blackshaw and Petrovskii 2007; Petrovskii and Blackshaw 2003).

2.2 Population data

Populations of *T. paludosa* larvae in Scottish farmland were surveyed annually (usually in January/February) between 1975 and 1994. The results as a whole remain unpublished, a part of the data was earlier used by Blackshaw and Petrovskii (2007). Population counts were obtained from soil cores extracted from individual fields (20 cores per field), which is a common technique for soil zoology (cf. Mayor and Davies 1976). The details of sampling (such as the time of sampling, the core's volume etc.) were consistent across the survey and as such all counts obtained are comparable. For each field, the mean number of insects per core was calculated and we assume that these numbers provide absolute estimates of the population levels at the time of sampling. A total of 83 fields were sampled over the course of the survey period. However, most fields were sampled for less than the full twenty years. In particular, sampling did not begin in the same year for all fields. Furthermore, not all of the time series are complete for the period studied;

for some years, the count is not available.

The purpose of this study is to investigate the synchronisation of local populations, i.e. the populations in individual fields. In order to obtain a detailed view of the spatial aspect, it is desirable to include as many fields as possible. On the other hand, the accuracy of estimates of the degree of synchronisation will be dependent on the length of the time series used. Consequently it is preferable both that time series cover the greatest duration possible and that as many different time series as possible are used.

Given these limitations, it is not possible to use all fields surveyed. A compromise between number of fields and length of time series has to be found. Consequently, we restrict our analysis to a subset of 38 fields for which a complete fifteen year time series between 1980 and 1994 is available. A map of the fields in question can be seen in Fig. 1.

Information about the minimum, maximum and time-average size for each of the local populations (as represented by the mean value across the collected soil cores, see above) is given in Tab. 1. It is readily seen that the populations exhibit considerable variability. More detailed data on the *T. paludosa* population size in five particular fields over the given period, 1980-94, are shown in Fig. 2. A visual inspection of the data reveals a certain degree of correlation between the time series, such as, for instance, a decrease in all five population sizes between 1987-88, a minimum population size in 1985 and 1993 (three out of five fields), an increase in the population size between 1993-94 (four out of five fields), etc. A quantitative insight into this is made below.

2.3 Elimination of population density dependence

Ninety-seven percent of the populations included in the study (i.e. 37 out of 38 fields) display significant population density dependence when subjected to the test outlined by Pollard et al. (1987). The effects of this density dependence on local population dynamics may obscure the effects of synchronisation between these populations. Consequently it is desirable to eliminate these density dependent effects from the local population dynamics.

The following model:

$$\Delta N_t = N_{t+1} - N_t = N_t \left[10^{\alpha} \left(\frac{\overline{N}}{N_t} \right)^{-\beta} - 1 \right] \tag{1}$$

(where $\overline{N}$ is the average population across the entire study area and α and β are to be

determined), which we write as

$$N_{t+1} = f(N_t) = N_t \cdot 10^{\alpha} \left(\frac{\overline{N}}{N_t} \right)^{-\beta}, \tag{2}$$

was introduced by Blackshaw and Petrovskii (2007) to describe these effects.

The parameters α and β can be determined by linear regression of $\log((\Delta N_t/N_t)+1)$ against $\log(N_t/\overline{N})$ for a given time series. Density dependence is expected to be a species property and as such the same parameters apply for each individual population. Thus we determine these parameters for the time series obtained by computing the average

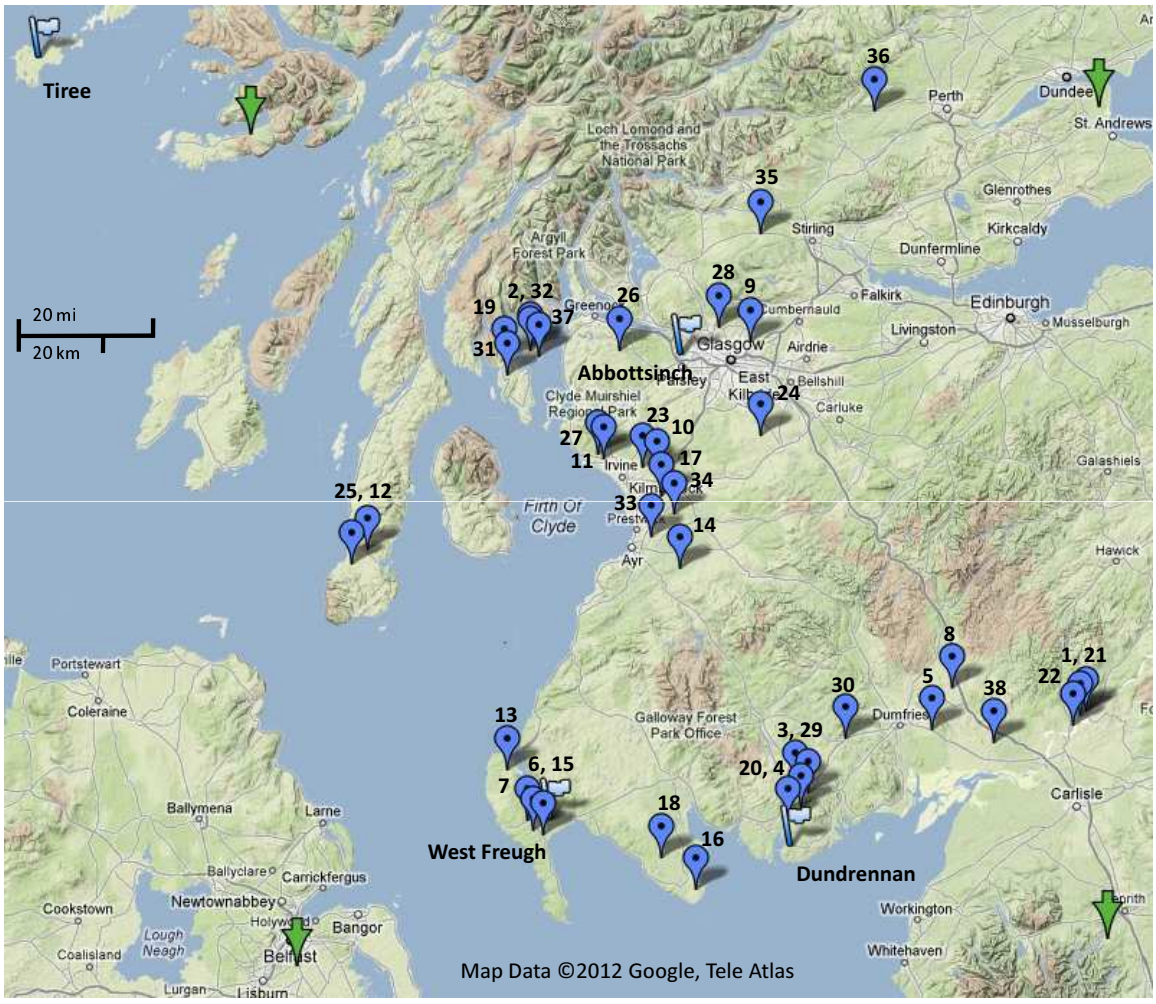

Figure 1: Map showing the locations of fields, indicated by balloon markers, included in this study. Numbers correspond to those in Tab. 1. The flag markers show the positions of weather stations from which data were obtained. The arrows provide an approximate location of the corner points of the plots used in Sections 3.4-3.5 (Figs. 8 to 11). Barren and rocky areas are shown in various shades of brown, while green shading is an indicator of grass cover. Relative height of terrain is indicated by the three dimensional effect.

Table 1: Minimum, maximum and the time-average of population counts for each field. Field numbering corresponds to that used in Fig. 1.

Num	Grid Ref	Min	Max	Average	Num	Grid Ref	Min	Max	Average
1	NY 416779	0	16	4.33	20	NX 693537	0	16	4.07
2	NS 114668	2	41	12.33	21	NY 426783	0	16	6.80
3	NX 716619	0	13	3.67	22	NY 394758	2	21	7.07
4	NX 724573	0	15	3.93	23	NS 369400	0	25	6.00
5	NY 049748	0	22	4.73	24	NS 659469	1	48	9.53
6	NX 071534	2	23	6.93	25	NR 661199	0	16	5.60
7	NX 057556	1	24	6.53	26	NS 324683	0	20	3.93
8	NY 101852	0	11	2.20	27	NS 265446	0	32	11.53
9	NS 639691	0	23	4.13	28	NS 562727	1	17	6.33
10	NS 402392	0	13	3.53	29	NX 743601	0	17	4.60
11	NS 278435	1	20	8.07	30	NX 839734	0	20	4.47
12	NR 698229	0	12	6.33	31	NS 053638	1	41	12.27
13	NX 008680	0	33	5.53	32	NS 111703	1	32	8.20
14	NS 452152	2	15	7.73	33	NS 385235	1	36	7.93
15	NX 093520	0	8	4.07	34	NS 440289	0	20	6.00
16	NX 463378	0	24	9.47	35	NS 671956	0	34	6.73
17	NS 412331	0	27	6.60	36	NN 943236	0	8	2.33
18	NX 377452	0	11	4.53	37	NS 129682	0	23	5.67
19	NS 046674	1	24	8.87	38	NY 203711	0	24	6.47

population across all fields at each time point. The resulting data are plotted in Fig. 3. Note that the resulting values of α and β correspond well to those obtained in previous studies (Blackshaw and Petrovskii 2007).

Now for each time series of populations, X, we can compute the difference between the observed and predicted populations for any time point as follows:

$$R_t^X = X_t - f(X_{t-1}), \tag{3}$$

(where $t = 2, 3, \ldots, n$) to obtain a time series of residuals, R^X, one time step shorter than the original observed data. These residuals measure the degree to which real populations deviate from the levels predicted by the density dependent mechanism either by chance

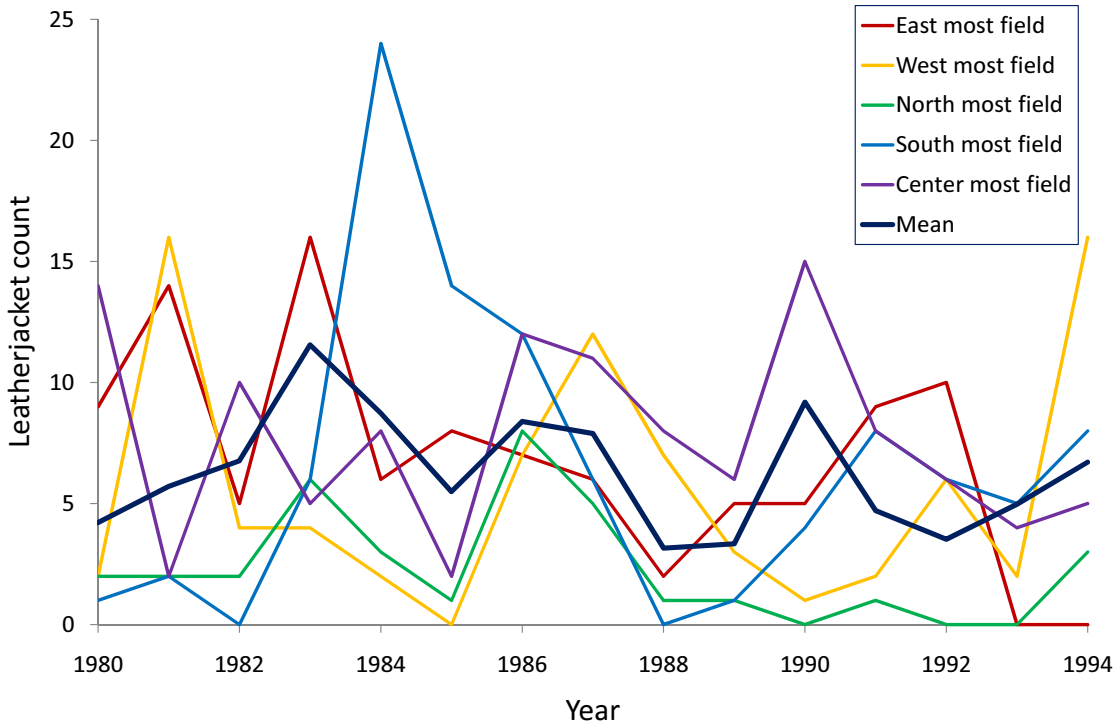

Figure 2: Plot of population counts against time for five example fields. Fields were chosen on the basis of geographic position; specifically, four are on the edges of the study area (field no. 36 at the North, no. 21 at the East, no. 16 at the South and no. 25 at the West) and the fifth is in the centre (field no. 14). The mean count across all thirty-eight fields in the study was determined for each year and is also plotted (black line).

or due to underlying processes which are not described by internal population regulation.

A histogram of all such residuals was constructed, see Fig. 4 (left), which strongly suggested that the residuals arise from a log-normal distribution. To confirm this intuition, a Q-Q plot of the residual distribution against the log-normal distribution was constructed, $\mathcal{LN}_R = \exp(\mathcal{N}(1.9, 0.537)) - 7.217$; see Fig. 4 (right). It is clear that the majority of the quantiles plotted lie on the line $y = x$ so the residual distribution is approximately given by the log-normal distribution stated.

Thus we can describe the population dynamics of these populations with the following stochastic difference equation:

$$N_{t+1} = \begin{cases} f(N_t) + \eta_R, & \text{if } f(N_t) + \eta_R > 0, \\ 0, & \text{otherwise,} \end{cases} \tag{4}$$

where η_R is a random variate drawn from the distribution $\mathcal{LN}_R$.

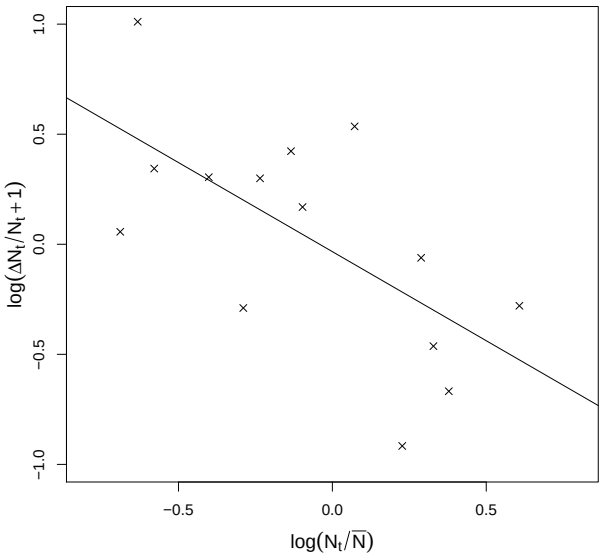

Figure 3: Log-log plot of the average per capita population increase against average relative population (crosses). The solid line was obtained by linear regression analysis of these data and has the intercept $\alpha = -0.0335$ and the slope $-\beta = 0.8903$. The R^2 value of this regression is 0.42.

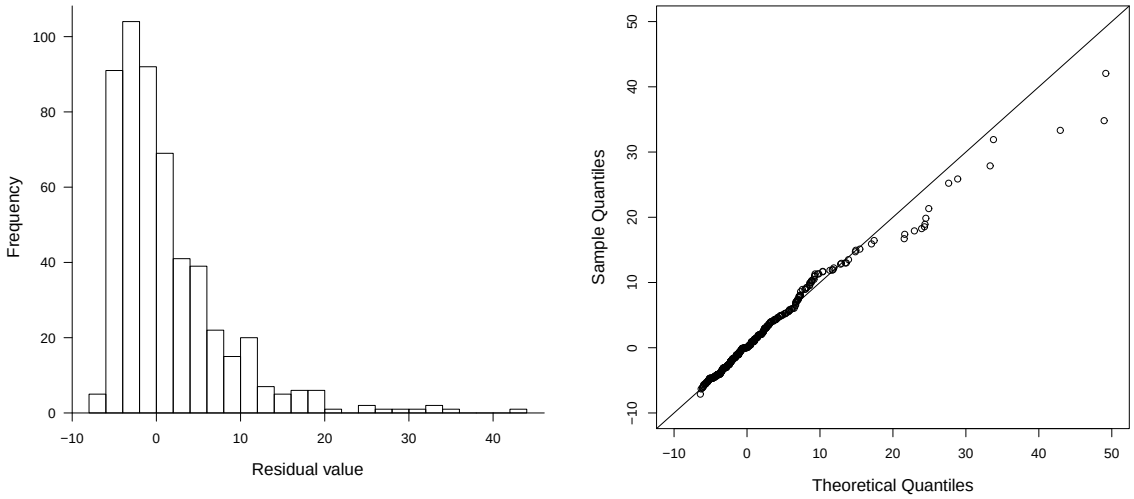

Figure 4: Left: Histogram of residuals as obtained after removing density dependence from the original data; see Eq. (3). Right: Q-Q plot of the residual distribution against the log-normal distribution given by $\exp(\mathcal{N}(1.9, 0.537)) - 7.217$.

2.4 Finding relationships between the local populations

We quantify the degree of synchronization between the populations of two fields (say, X and Y) by calculating the Pearson product-moment correlation coefficient of their respective residual time series, R^X and R^Y. This value is given by the following expression:

$$r_0(R^X, R^Y) = \frac{\sum_{i=2}^{n}(R_i^X - \mu_R^X)(R_i^Y - \mu_R^Y)}{\sqrt{\left(\sum_{i=2}^{n}(R_i^X - \mu_R^X)^2\right)\left(\sum_{i=2}^{n}(R_i^Y - \mu_R^Y)^2\right)}} \ , \tag{5}$$

where R_i^X and R_i^Y are the residual population densities at year i in fields X and Y, respectively, and μ_R^X and μ_R^Y are the sample means of the two time series, i.e.,

$$\mu_R^X = \frac{1}{n-1}\sum_{i=2}^{n} R_i^X \ , \qquad \mu_R^Y = \frac{1}{n-1}\sum_{i=2}^{n} R_i^Y \ . \tag{6}$$

It is not immediately clear, however, what constitutes a statistically significant correlation coefficient. Since we work with time series of finite length, and the data are affected by stochastic factors, any given value of the correlation coefficient (5) may appear by chance. One must therefore distinguish between the cases when high absolute values of $r_0(R^X, R^Y)$ are superficial and the cases when these values are the result of actual synchronization. In order to do so, the population data were subjected to a careful statistical analysis; full details of the analysis are given in the online Appendix.

2.5 Assessing the effects of time delay

The correlation coefficient (5) is not capable of fully explaining all possible relationships between two field populations. For example, if the fields are coupled by dispersal, then the corresponding biological mechanisms may be subject to time delay. The population census during the survey was done in winter, i.e. before the species enters its mobile (flying) stage. Therefore, the effect of dispersal coupling, if any, will only be seen in the next year census.

Obviously, the effects of delay are not taken into account by the standard correlation coefficient r_0. In order to identify such relationships (for a single generational delay of one year), we introduce a delay-based correlation coefficient which is calculated between two time series, A and B, as follows:

$$r_1(A, B) = \frac{\sum_{i=1}^{n-1}(A_i - \mu_{A,1})(B_{i+1} - \mu_{B,1})}{\sqrt{\left(\sum_{i=2}^{n-1}(A_i - \mu_{A,1})^2\right)\left(\sum_{i=2}^{n}(B_i - \mu_{B,1})^2\right)}} \ , \tag{7}$$

where $\mu_{A,1}$ and $\mu_{B,1}$ are defined as follows:

$$\mu_{A,1} = \frac{1}{n-1}\sum_{i=1}^{n-1} A_i \ , \qquad \mu_{B,1} = \frac{1}{n-1}\sum_{i=2}^{n} B_i \ . \tag{8}$$

We emphasize that, generally speaking, $r_1(A,B) \neq r_1(B,A)$. Therefore, the delay-based correlation coefficient separates the effect that the populations of field A have on field B (described by $r_1(A,B)$) from the effect that the population of field B may have on A (described by $r_1(B,A)$). In other words, it takes into account a possible asymmetry in the inter-field coupling. Such asymmetry can occur, for instance, when insect dispersal is assisted by the wind (Gatehouse 1997; Compton 2002) in case wind has a prevailing direction. This kind of asymmetry reflects what is essentially a traveling wave as has been observed in the dynamics of childhood diseases (Rohani et al. 1999).

It remains then to determine which time series this coefficient should be calculated for. An immediate analogue of the comparison used in the undelayed case would use $r_1(R^X, R^Y)$. This would then compute the degree to which deviations from internal dynamics of one population affect deviations from the internal dynamics of another population. However, here we argue that this is not a meaningful measurement. Instead we are interested in how the absolute population in one location (regardless of whether it is higher or lower than internal dynamics would predict) may affect the population dynamics at another location. The strength of this relationship should be described by the value of $r_1(X, R^Y)$[2]. Note that in this case the asymmetry lies not only in the correlation coefficient but in the series which are compared.

3 Results

3.1 The effect of distance on strength of correlation

Several earlier studies have shown that there exists a clear "synchrony versus distance pattern" where the correlation between population abundances tends to decrease as the distance between the populations increases (Sutcliffe et al. 1996; Lundberg et al. 2000; Peltonen et al. 2002). A reasonable initial hypothesis therefore seems to be that populations in fields which are close together are more likely to exhibit synchronization than populations that are spatially more separated. In order to investigate this hypothesis,

[2] Values computed in this way are referred to as r_1 from now on.

the correlation coefficients obtained for each pair of fields are plotted against the distance between the fields; see Fig. 5, top-left for r_0 (no time delay), top-right for r_1 (time delay of one year).

A visual inspection, however, does not reveal any clear pattern. We observe that, indeed, some fields are strongly synchronized up to distance of 150-170 kms; this happens both with and without time delay. There are also fields that are significantly anti-

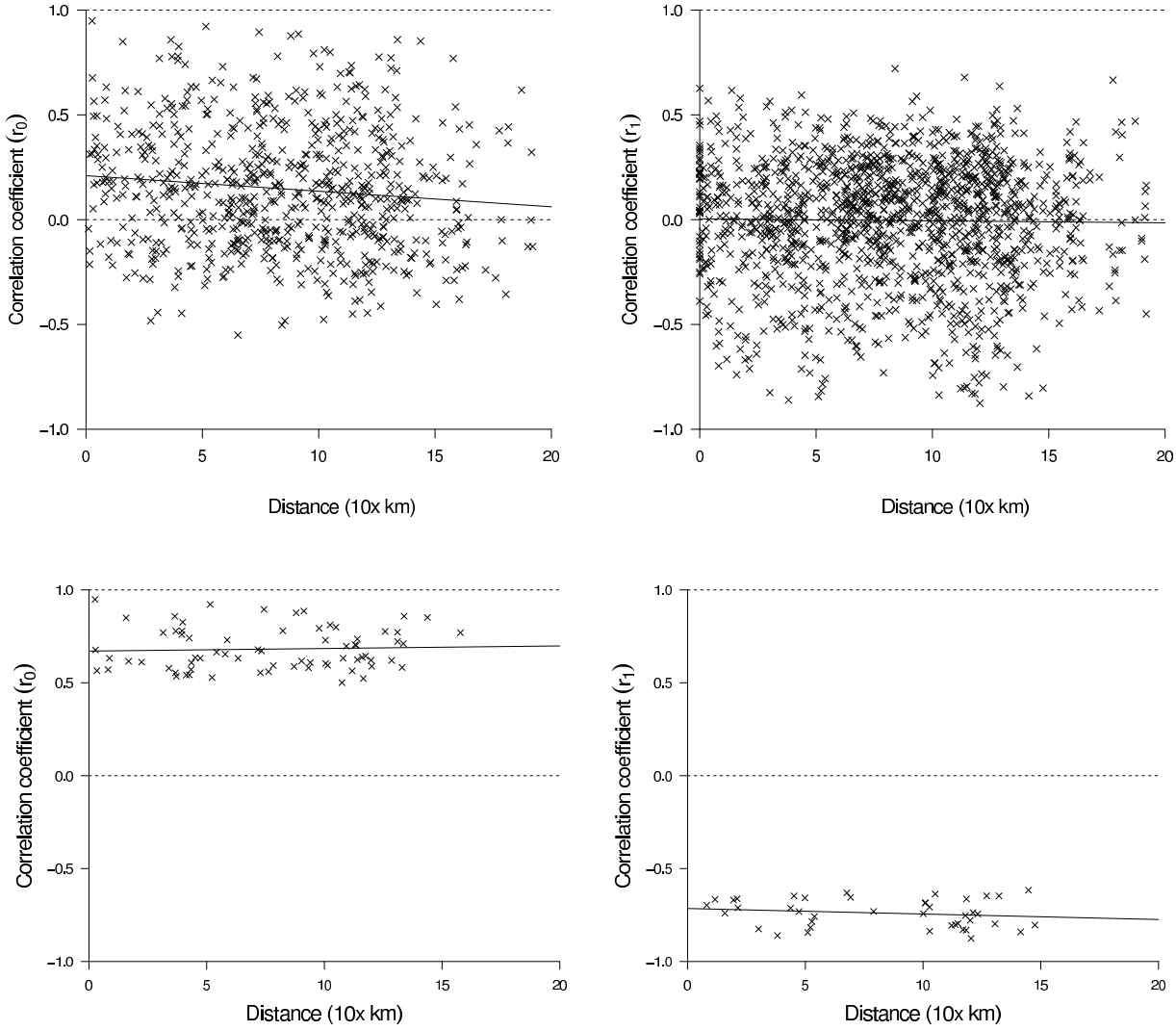

Figure 5: Plots of correlation coefficients for pairs of distinct fields against distance between those fields. The top-left plot shows all the correlation coefficients calculated without a time delay (as given by Eq. 5), the top-right plot uses a time delay of 1 year (Eq. 7). The bottom row show the correlation coefficients that are statistically significant at 5% level, left without time delay, right with a delay of 1 year. The solid lines indicate trends predicted by linear regression analysis.

correlated. On the other hand, for any inter-field distance (including the cases of apparent proximity), there are fields that are not correlated at all. On the whole, the plots for r_0 and r_1 are broadly similar[3], although stronger negative correlations are observed for the time delay case. We therefore conclude that, as such, the absolute distance between fields cannot be the only controlling factor in whether the populations of two fields synchronize. Hence, more information about the 'geometry' of the environment has to be taken into account.

This qualitative understanding can be made more rigorous using linear regression analysis. The results are plotted as solid lines in Fig. 5. Interestingly, the regression analysis of correlation with respect to distance reveals different behaviour between the two cases. In the no-delay case, the correlation strength shows a tendency to decrease as distance increases. The gradient of the slope is small (approximately -0.0074), but statistically significant with a p-value below 0.01. The correlation coefficient predicted by the best-fitting line is about 0.2 at small distances and it approaches zero for distances on the order of 300 kms. In the time-delay case, the correlation strength is not significantly different from 0 for any distance range.

The existence of the inter-field coupling over the whole area becomes even more evident if the correlation-versus-distance analysis is restricted to statistically significant values only. The results are shown in the bottom row of Fig. 5. In the no-delay case all the significant correlation coefficients appear to be positive and have a relatively large value between 0.5 and 1.0 (Fig. 5, bottom, left). In the time-delay case, all the statistically significant correlation coefficients are large and negative (Fig. 5, bottom, right). Surprisingly, in neither of the two cases does the correlation strength show any decay with distance; on the contrary, the two best-fitting lines have gradients of 0.001 and -0.0029 respectively, but these values are statistically not significantly different from zero.

3.2 The effect of direction on strength and sign of correlation

In the previous section, we showed that the population dynamics of *T. paludosa* in the study area is synchronized over large distances, although the inter-field distance alone provides a rather poor description of the synchronization pattern, especially in the time-delayed case (see Fig. 5, top, right). More details of the synchronization pattern can be obtained if we consider the relative positions of fields whose populations are correlated.

[3]Note that the time delay case includes twice as many points as the no delay case.

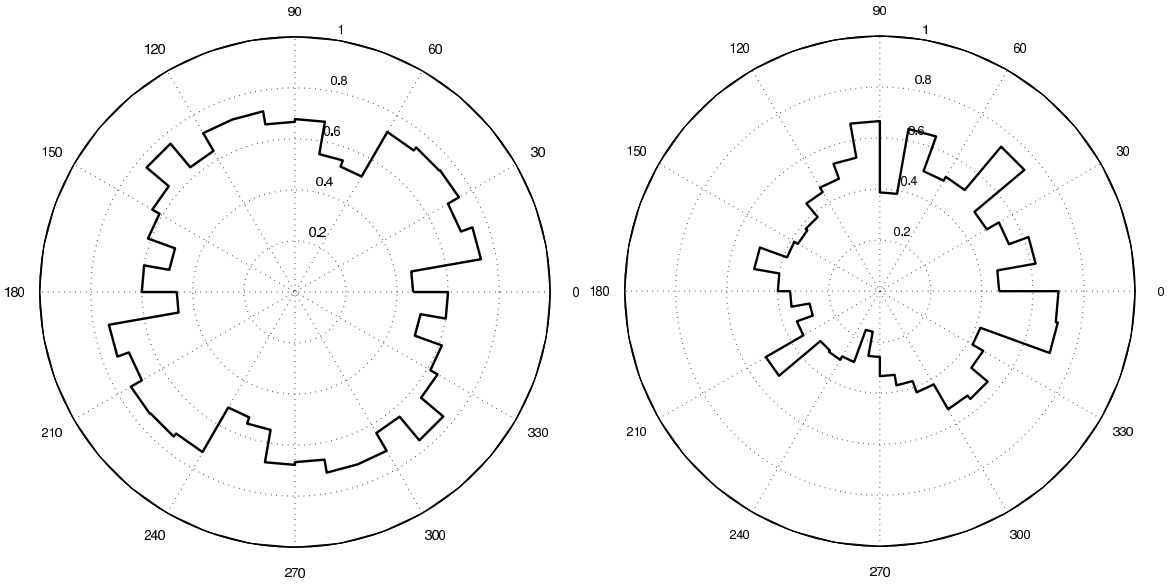

Figure 6: Relative frequency of positive and negative correlations as a function of bearings between fields. Left: positive correlation without time delay between residual populations, Eq. (5). Right: negative correlation with a one year time delay between population and residual population, Eq. (7). The radial distance between the center of the circle and the thick broken line gives the relative frequency of positive (left) or negative (right) correlations (as a fraction of unity) within the given bearing range; see details in the text.

This can be described in part by the directions of the lines connecting any pair of fields, i.e. by considering the bearing of one field from another.

A quantitative insight into how relationships between populations vary with respect to bearing can be made by considering the relative frequency of positive and negative correlation values in a given bearing range. That is given a bearing range, 0-10° for example, we divide the number of positive (or equivalently negative) correlation values obtained in that range by the total number of correlation values obtained in that range. The resulting histograms for correlations computed with and without a time delay are shown on a unit circle in Fig. 6. Note that, in order to take into account the different tendency observed in the delayed and non-delayed cases (as seen from Fig. 5, top), for r_0 we present the fraction of positive correlations obtained, while for r_1 we present the fraction of negative correlations obtained.

It is readily seen that, when no time delay is considered, the relative frequency of positive and negative correlations is approximately independent of bearing, and positive relationships (shown by the thick solid line in Fig. 6, left) are clearly more common over

the whole circle. In contrast, when a time delay is introduced, the relative frequency of positive and negative correlations is strongly dependent on the bearing between the fields. Negative correlations (shown by the thick solid line in Fig. 6, right) prevail in the range of bearings between south-east and due north, while in the remainder of the range positive correlations dominate. We therefore conclude that the synchronization pattern has a clear directional aspect.

3.3 Analysis of weather pattern

Weather conditions are known to have a significant impact on the population dynamics of many insect species (Baars and Van Dijk 1984; Williams and Liebhold 1995; Raimondo et al. 2004). In particular, the direction and strength of the wind were proved to be factors strongly affecting dispersal of flying insects (Gatehouse 1997; Compton 2002). Aiming to explain the observed directional asymmetry in the synchronization pattern, we therefore now turn our attention to the weather pattern. Indeed, synchronization between local populations is known to result from either the Moran effect or dispersal coupling between habitats. It seems improbable that the regional stochasticity (e.g. short-term stochastic variation in the local temperature and humidity) could possess a directional aspect. In contrast, the existence of a prevailing wind direction, if any, obviously can make the coupling asymmetric.

Measurements of wind velocity were recorded at four weather stations spanning the study area (see Fig. 1), i.e. Dundrennan, Abbottsinch, West Freugh and Tiree. The time series are obtained from a single year, 1987, which we assume to be representative for the whole duration of the survey. The data cover a two month period, August to September. This period corresponds to peak adult emergence of *T. paludosa* and thus is the time in which interactions between dispersed populations are most likely. The data[4] comprised hourly measurements of the average wind speed and the wind direction.

Some signs of environmental heterogeneity within the study domain can be immediately identified from the distributions of average windspeed; see Fig. 7. The weather stations at West Freugh and Tiree tend to report higher windspeeds than the less exposed stations at Dundrennan and Abbottsinch, presumably because higher windspeeds can be sustained over the relatively flat surfaces of the surrounding seas and wide stretches of water. In contrast, the wind direction appears to be less influenced by local terrain as is shown by

[4]Original data supplied by the Met Office; http://www.metoffice.gov.uk

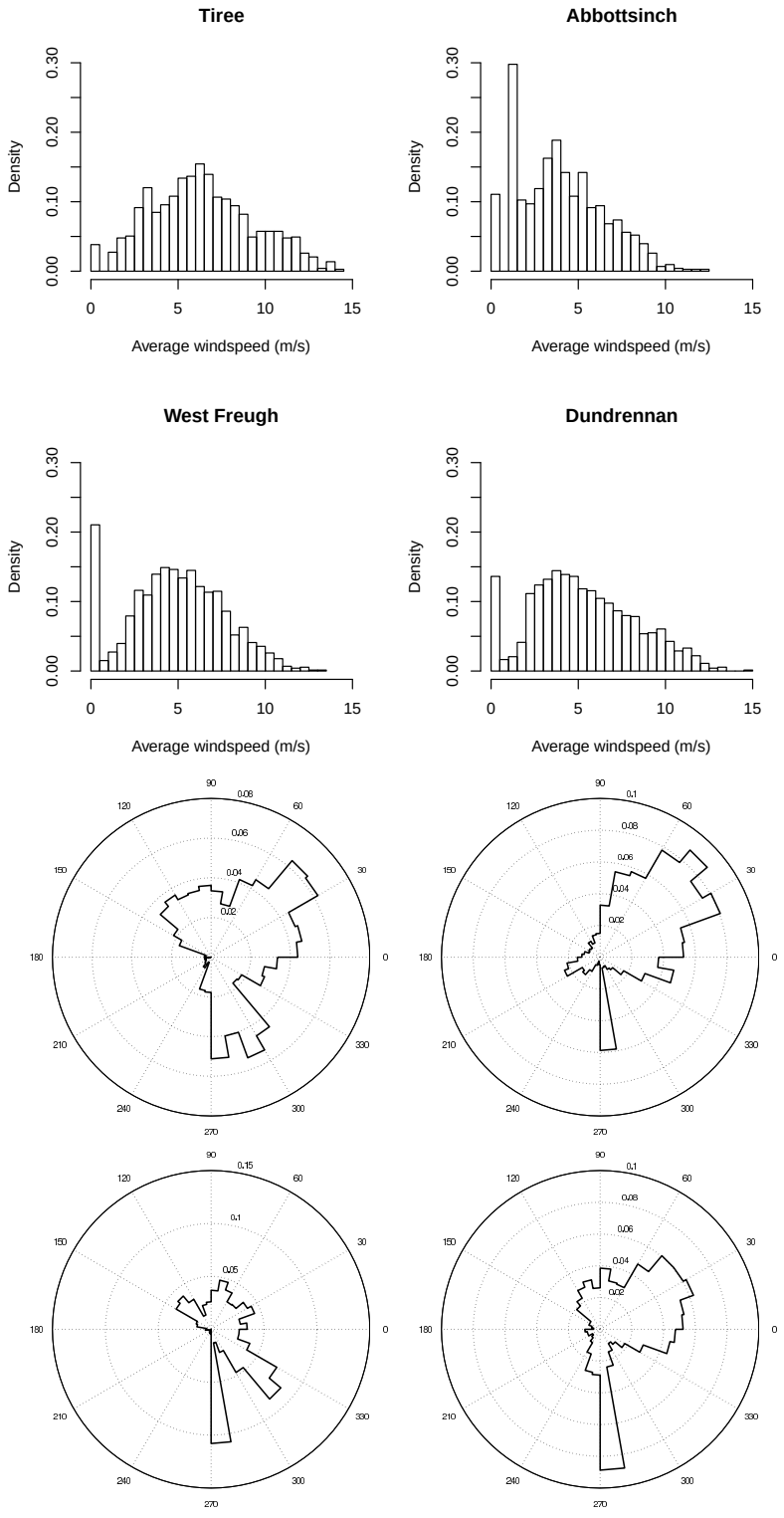

Figure 7: Histograms of average wind speed and wind direction over the study period at four weather stations. Wind direction histograms are in polar form and are laid out in the same order as those of average wind speed.

the comparison between Fig. 7 and Fig. 1. The stations at West Freugh, Abbottsinch and Dundrennan suggest that winds predominantly blow either due south or between south east and north, at Tiree the separation between these two modes is less pronounced. In general, there is very little wind blowing in the south to north-west sector. This is in strikingly good agreement with the pattern shown in Fig. 6, right.

3.4 Spatial cross-correlations with no time delay

In Sections 3.1 and 3.2, we quantified the cross-correlations between fields by pooling all correlations together. In particular, the existence of correlations between the local populations (with no time-delay) across the region "on average" was shown by finding the best-fitting line to the whole array of pairwise correlation coefficients versus distance;

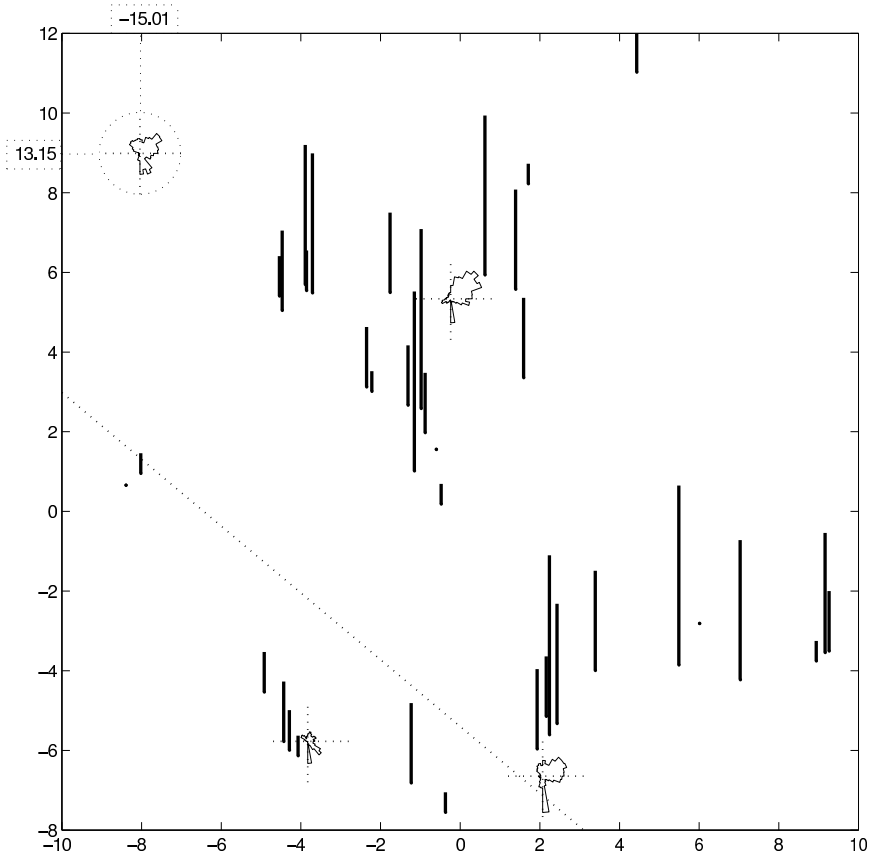

Figure 8: The height of the bar at a given field indicates the number of populations with residuals significantly correlated to that field's residual population (ranging from between 0 and 10); further details are given in the text. The labels on the axes shows relative position in tens of kilometers. The inset (top-left corner) shows a weather station that is situated outside of the domain.

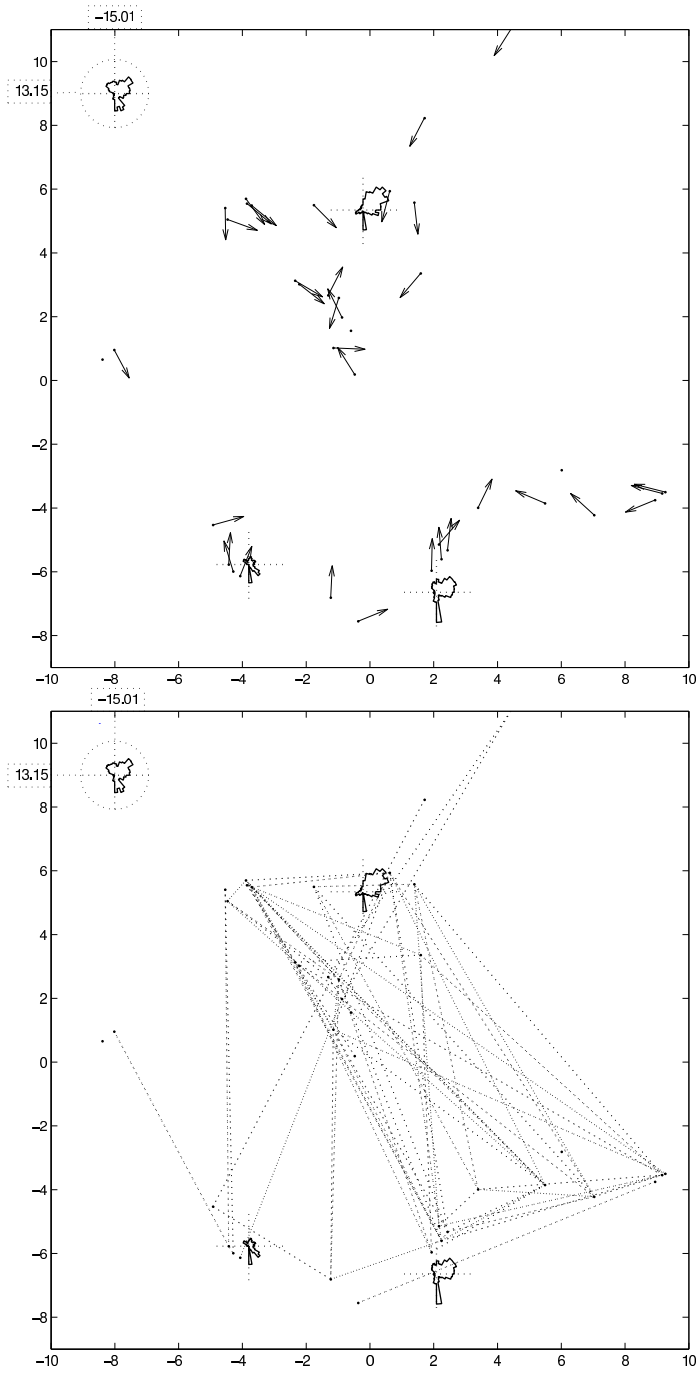

Figure 9: Top: The arrow at a given field indicates the average direction to fields with residual populations that are significantly correlated to the resident residual population. Bottom: The dotted lines connect fields with significantly correlated residual populations. Further details are given in the text. Scales indicate relative position in tens of kilometers. The inset (top-left corner) shows a weather station that is situated outside of the domain.

see Fig. 5, left. The existence of a directional aspect (to the time-delayed relationships) was revealed by plotting a histogram of (weighted) correlation coefficients on a circle, i.e. as a function of the bearing (Fig. 6). However, these cumulative properties obscure the role of individual fields. Meanwhile, revealing the contribution of individual fields may be important for better understanding the process behind the observed pattern. The contribution from different pairs of fields to the "synchronization vs distance" pattern, as given by Fig. 5, varies significantly regardless of the distance between them, and hence one might wish to understand why. Besides, the terrain in the study region is highly heterogeneous. It includes hills, valleys, plains, urban areas, as well as some considerable stretches of water (e.g. Firth of Clyde). Different local populations are therefore exposed to quite diverse environments that vary both in terrain and in weather conditions.

In order to analyse the impact of precise positional relationships between fields, we now consider all fields individually. In this section, we consider the correlations calculated without time delay (see Eq. 5). The results are summarized in Fig. 8. For each given field X, we count the number of the fields where the residual population dynamics of *T. paludosa* is significantly correlated (at the 5% significance level) to the residual population dynamics in X. Note that, in this case, all the significant correlation coefficients had positive sign; see Fig. 5 (bottom, left). The result is shown by the length of a bar based at the location of each field. The shortest bar (with the length 0.5 unit on the map scale) means that one other population is significantly correlated to this population. The largest number of fields significantly correlated to a given one is found to be 10 (with the length of the corresponding bar thus being set to 5 in map units). For the three fields that do not have a significant correlation to any other field in the array, the bar has length 0, and so their position is shown by a dot.

It is readily seen that the map shows a clear divide between parts of the region above and below the dashed line (which has been included for ease of comparison). In the North-East region, above the dashed line, most of the populations are correlated with a large number of other populations (4.27 on average). In contrast, in the South-West region, below the dashed line, populations are correlated to significantly fewer populations (1.75 on average).

The information shown in Fig. 8 is, however, incomplete until the position of the mutually correlated fields is known. Consider a hypothetical case that field X is significantly correlated to fields A, B and C; one then might wish to know where fields A, B and

C are situated with respect to X. Figure 8 is therefore complemented with Fig. 9. In the top plot in Fig. 9, the arrows (now normalized to a unit length) indicate the average direction to all fields (say, A, B and C) whose populations are significantly correlated to that in the given one (say, X). If a given field is correlated to just one other field, then the corresponding arrows point towards each other. In the lower plot in Fig. 9, any significant relationship between two populations is indicated by a dotted line. Whereas the upper plot can be considered a summary of the relationships between a field and the remaining populations, the lower plot provides an overview of the networks of relationships formed between these populations. Since the weather conditions are expected to be important, in order to give a visual idea about the impact of the wind velocity, the position of each weather station is indicated by the intersection of two dashed lines. The solid lines originating from this intersection replicate the histograms of wind direction given in Fig. 7. Interestingly, apart from a few exceptions, the strongly correlated fields in the North East region appears to be mostly correlated between themselves forming a dense network which largely exlcudes fields in the South West. The fields in the South-West region form a similar, if more sparse, network, with limited interconnections with the North-East network. This provides further evidence of the existence of a division between the North-East and South-West regions.

The results shown in Fig. 9 confirm that geographical proximity does not appear to be a factor controlling what fields are correlated. It is readily seen that there are many situations when a field is not correlated to its immediate neighbour(s) but is significantly correlated to fields much further away.

3.5 Spatial cross-correlations with a time delay

In the previous sections, we have shown that the standard correlation coefficient (5) is not able to describe all possible relationships between two fields; e.g. see Figs. 5 and 6. A dispersal mechanism is likely only to be detected when a time delay is introduced between two populations. An analysis of the relationships between influencing populations and influenced residual populations with a generational delay (of a single year in this case) can be performed in a similar way to that presented in the last section. Again we limit our attention to those relationships which are significant at the 5% level. The plots below, see Figs. 10 and 11, are therefore analogous in concept to Figs. 8 and 9.

As we previously observed, the time delay introduced in (7) breaks the symmetry

implicit in the standard correlation coefficient (5). Consequently it is possible to consider two classes of relationships between a given population and the other populations. The first class is the set of residual populations which, when delayed by one year, are correlated to a given population, i.e. the set of populations influenced by a given population. The second class is the set of populations which are correlated to a given residual population when it is delayed by one year, i.e. the set of populations influencing a given population.

In Fig. 10, the number of populations influenced by and influencing a given field population is shown by, respectively, the length of a bar above and below the field position (indicated by a plus sign). The scale of these bars is as described in the previous section. Note that, in contrast to the relationships presented in the previous section, all of the statistically significant time lagged relationships now have negative coefficients; see Fig. 5 (bottom, right).

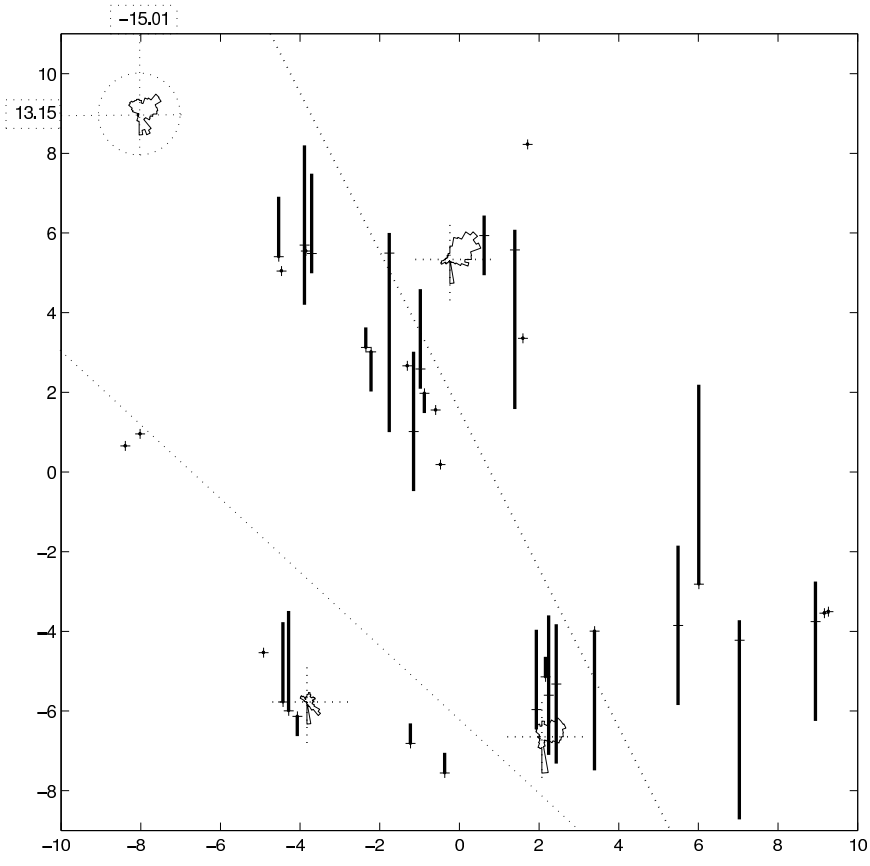

Figure 10: The length of the bar descending (rising) from a given field position indicates the number of fields with populations significantly influencing (influenced by) that field. Further details are given in the text. Scales indicate relative position in tens of kilometers. The inset (top-left corner) shows a weather station that is situated outside of the domain.

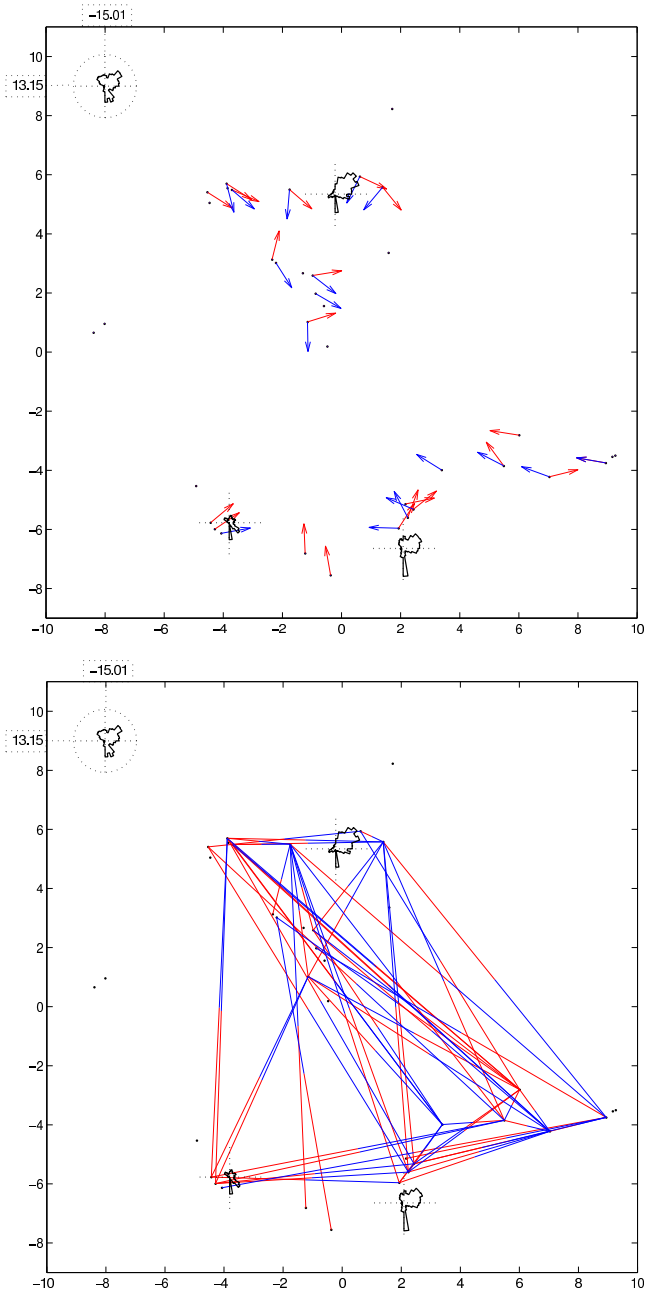

Figure 11: Top: The red arrow at a given field indicates the average direction to all fields whose residual populations are significantly influenced by that field. The blue arrow corresponds to the average direction to all fields whose populations have a significant influence on that field's population. Bottom: The dotted lines connect fields between which significant relationships exist. The red section of each line emanates from the influencing field, the blue section terminates at the influenced field. Further details are given in the text. Scales indicate relative position in tens of kilometers. The inset (top-left corner) shows a weather station that is situated outside of the domain.

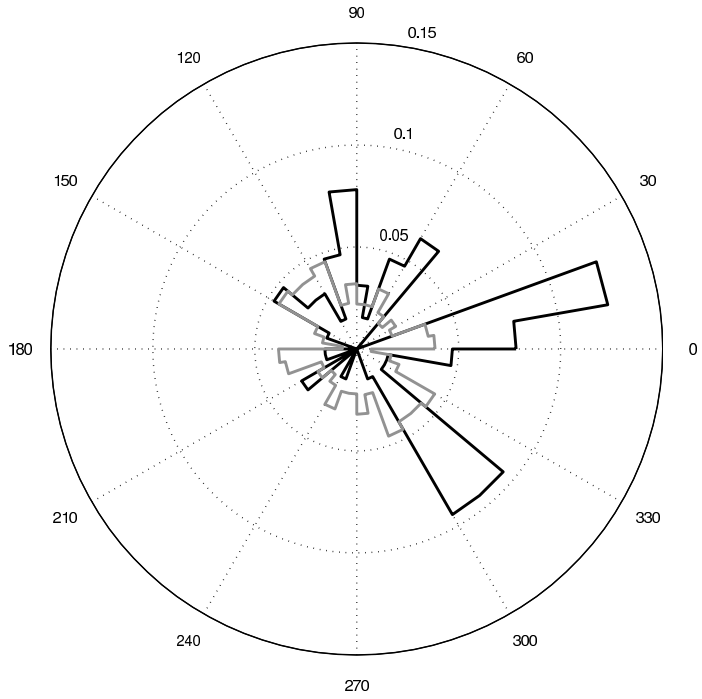

Figure 12: Distribution of bearings from significantly influencing to influenced populations represented as a histogram. The solid black line indicates the density of significant bearings in the range shown. The solid gray line shows the overall distribution of bearings within the study area.

As in the previous section we add reference lines to divide the study area into three regions, referred to as South-West, Central, and North-East. The average number of fields influenced by a population in any given region is (approximately) constant across the three regions, with values of 1.38, 1.94, and 1.54 in the South-West, Central and North-East regions respectively. In contrast the average number of populations influencing a given population varies significantly across these regions taking values of 0.125, 1.12 and 3.38 in the South-West, Central and North-East regions respectively. Thus populations in the South-West are more likely to influence other populations than to be influenced themselves while populations in the North-East show the opposite trend. Populations in the Central region influence other populations and are influenced themselves at roughly equal levels.

Similarly to the previous section, we complement these data with plots showing the directions between fields and the populations that they influence or are influenced by, Fig. 11. In the top plot of this figure red arrows indicate the average direction to residual populations which a given population significantly influences. Blue arrows indicate the average direction to populations which significantly influence a given residual population.

In the lower plot all significant relationships are represented by a two colour line connecting the fields between which the relationship exists. The red section of this line connects to the influencing field while the blue section of the line connects to the influenced field.

Including the positional information in our analysis of this pattern again produces further understanding. The strong correlations within regional groupings observed in the undelayed case are, for the most part, absent. Instead South-West populations appear to influence Central populations which in turn influence North-East populations in an apparent cascade; see, for example, the relationships between fields along the southern edge of the study area. Similar interactions can be seen between the populations of the northern corner and those to their south-east although it is less pronounced.

The distribution of bearings from significantly influencing to influenced is presented as a histogram in Fig. 12 (black line). It is clear that this distribution deviates noticeably from the underlying distribution of bearings between fields in the study area (shown by the grey line); therefore, the observed directional asymmetry cannot be reduced to the effect of the system geometry. The most significant deviations from this underlying distribution lie between south east and north. Since all of these relationships have negative correlation coefficients this is in good agreement with the trend observed in Fig. 6. Furthermore, it corresponds well to the pattern shown in Fig. 11.

4 Discussion and Conclusions

In this paper, we have considered the population dynamics of an insect pest, *T. paludosa*, on a habitat consisting of 38 agricultural fields in South-Western Scotland. The annual data on population abundance collected in a survey accomplished during 1980-94 were analysed. Our goal is threefold. Firstly, we want to reveal whether there is a correlation between the fluctuations in local populations, the phenomenon known as synchronization (Lundberg et al. 2000; Liebhold et al. 2004). Secondly, we want to reveal the corresponding spatial pattern, i.e. how the degree of synchronization between fields changes in space, in particular, with inter-field distance. And thirdly, we want to understand the process(es) resulting in the observed synchronization pattern, i.e. to relate the observed properties of the *T. paludosa* metapopulation to a specific mechanism or factor.

The first goal is relatively simple to reach. We have calculated all cross-correlation coefficients as given by r_0, see Eq. (5), and found that only a small fraction of fields is

uncorrelated or weakly correlated (say, $|r_0| < 0.1$). A majority of population pairs are positively correlated, in many cases r_0 being as large as 0.5 or even higher (see Fig. 5, top, left). There is also a considerable number of pairs that are negatively correlated with typical values of r_0 between -0.1 and -0.3.

With regard to the spatial pattern, no matter whether synchronization is due to dispersal or the Moran effect, it is reasonable to suppose that the cross-correlation coefficient should decrease with the distance (e.g. Liebhold et al. 2004). We have shown, however, that this expectation is rather over-simplified. While the best-fitting line obtained by using the linear regression analysis indeed has a negative slope (see Fig. 5), a closer look at the correlation strength versus distance immediately reveals that this 'prediction' about the decay in synchronization is rather superficial. Instead, synchronization exhibits an intermittent behaviour: For any range of the inter-field distances, from very small (a few kms) to very large (up to 200 kms), there are fields that can be strongly positively correlated, negatively correlated or virtually uncorrelated. In case the analysis is restricted to the statistically significant correlations only (Fig. 5, bottom, left), the decrease in the correlation strength with distance is not seen at all, at least up to the scale of 200 kms.

Beside the usual cross-correlation coefficient r_0, we also calculated a delay-based cross-correlation coefficient r_1 as given by Eq. (7). Such a delay (assumed to be one year, i.e. one generation for *T. paludosa*) can arise if synchronization is induced by dispersal. Recall that the population data were collected in mid-winter, i.e. when the species is in its larval stage. Dispersal is however associated with the flying stage that normally happens in late August/early September. Therefore, the effect of dispersal will not be seen in the census until the next year. The effect of delay is likely to be felt more strongly if dispersal is asymmetric, i.e. field X delegates a fraction of its population to field Y but not vice versa. In contrast, synchronization due to the impact of stochasticity is unlikely to be subject to delay.

Interestingly, r_1 exhibits properties significantly different from r_0; see Fig. 5, right. The values of r_1 are predominantly negative, especially if the analysis is restricted to statistically significant values (Fig. 5, bottom, right) There is no decay with distance at all as the best-fitting line has a slope very close to zero. Contrary to r_0, the time-delayed coefficient r_1 show a clear directional aspect (Fig. 6, right) so that the relationship between fields appear to be stronger in the East-North-East and South-East directions than on other bearings (see Fig. 12). This is in good agreement with meteorological data on wind

direction, thus we suggest that dispersal is wind-assisted. Note that we are not able to provide a more quantitative proof of the impact of the wind on population synchronization, e.g. by calculating a correlation coefficient between the bearing of the pairwise correlations and the wind velocity. Such calculation would require high-resolution data on the wind direction across the whole study area; unfortunately, such data do not exist.

Note that from the whole range of environmental factors we only consider wind explicitly; regarding other factors as environmental stochasticity. Another relevant factor can be precipitation. However, rainfall only has a significant impact on the population abundance when autumn is exceptionally dry (Milne et al. 1965; see also Blackshaw and Petrovskii 2007) and there is no evidence of any abnormal precipitation level in South-Western Scotland during the period of study.

In this work, we have investigated the synchronization pattern obtained for a time lag of one year. This choice seems to be suggested by *T. paludosa* life traits. However, we have also considered longer time delays of two and three years. The corresponding cross-correlation coefficients r_2 and r_3 show the properties generally similar to those of r_1; in particular, the networks of inter-field connections (not shown here for the sake of brevity) have shapes which are only slightly different from that shown in Fig. 11, with a few links having disappeared and a few new links having emerged. A general tendency seen with an increase in time lag is a gradual decrease in the average correlation strength. The essential features of the time-lagged correlations are therefore encompassed by the coefficient r_1.

The differences between r_0 and r_1 can be used to distinguish between the contribution from dispersal and the Moran effect, which is the third goal of our study. We associate the no-delay coefficient r_0 with the effect of environmental stochasticity and the delay-based coefficient r_1 with dispersal. Since synchronization is seen both with and without time-delay, we conclude that both mechanisms are involved.

A counter-intuitive finding is that both mechanisms operate on approximately the same spatial scale of about 200 kms, as given by the size of the study area. With regard to dispersal coupling, it seems to be a surprising result as *T. paludosa* females are known to be poor flyers with typical dispersal distances thought to be below one hundred meters. For species with poor dispersal abilities, synchronization due to dispersal is thought to occur on a spatial scale much smaller than that of synchronization due to the Moran effect (Sutcliffe et al. 1996; Peltonen et al. 2002). However, this obviously does not account for

the potential impact of wind, which would not only provide a directional effect but also uncouple any dispersal-distance relationship at smaller scales. What can be true for forest insects, may not necessarily be true for insects dwelling on bare plains and hills of South-Western Scotland. With a wind speed of several meters per second (which is typical for the study area, see Fig. 7), the air flow is strongly turbulent. Turbulence creates ascending currents that can keep individual insects in the air[5] for many hours (taking also into account the complicated body shape and the relatively large wing-span of the cranefly), i.e. the time that is quite sufficient for them to reach another breeding ground situated a long distance away from their natal field. We note that, although direct evidence of wind-assisted dispersal for *T. paludosa* is not available, "sailing with the wind" is a typical dispersal strategy for many other insect species, with distances covered being dozens and even hundreds of kilometers (Gatehouse 1997; Compton 2002). We also note that the number of successfully travelling females does not necessarily need to be large. There is growing evidence that dispersal coupling by even a small fraction of the population may bring population fluctuations into synchrony (Haydon and Steen 1997; Kendall et al. 2000; Ripa 2000).

We also mention that there are some other mechanisms that may, in principle, synchronize the population fluctuations. Firstly, synchronization can emerge through interaction with another species that is itself synchronized (Liebhold et al. 2004). However, we are not aware of any species that exerts a consistent, regulatory effect on *T. paludosa* populations and so we consider this possibility the least likely explanation. Secondly, since *T. paludosa* is a pest, its abundance is controlled by pesticides. Should the application of pesticides be synchronized across the region, it could possibly synchronize the dynamics of the pest. However, the existing agricultural legislation in the UK does not impose on farmers any obligatory response to pest infestation. In fact, not only are pest controlling measures purely voluntary, but so too is participation in monitoring programs. The probability of a synchronized pesticides application is therefore rather unlikely.

Further evidence of the coupling by the wind-assisted dispersal may also be obtained by developing a more detailed theoretical framework operating across the whole range of spatial scales involved. Indeed, a comprehensive model of the dynamics of an individual population must take all the local populations into account. Correspondingly, it should

[5] *T. paludosa* have been caught in suction traps at 14 meters above ground in samples collected as part of the Rothamsted Insect Survey (Blackshaw, unpublished data).

take into account environmental processes acting on a regional scale along with those going on locally. In particular, such a model should make use of the patterns in directionality observed (e.g. see Fig. 12) in order to estimate the probability that a given population will be influenced by any other population in the study area. A functional relationship describing the effect of one population on another could then be derived in a similar way to that used to obtain Eq. (1) but weighted with the probabilities of given interactions with respect to distance and bearing. In conjunction with Eq. (1), this would provide a more complete description of a given population's dynamics region-wide. However, parametrization and verification of such a model can hardly be possible until the impact of wind and terrain are incorporated explicitly into these functional relationships. This is a complex task which clearly lies beyond the scope of this paper; in particular, more detailed weather data currently do not exist.

Given the evidence presented, the dynamics of apparently isolated populations of *T. paludosa* cannot be completely described by internal mechanisms (e.g. by density dependence). Instead, these dynamics are noticeably influenced by the dynamics of populations of this species at other locations. Results of our analysis indicate that the wind is likely to be a factor responsible for the inter-habitat coupling on the spatial scale up to 200 kms. This is rather counter-intuitive as *T. paludosa* are usually regarded as poor flyers. A study to look for genetic similarities between different populations across the whole area could confirm the existence of inter-habitat coupling by direct transport. We are considering undertaking such an investigation in the future.

Although in this paper we have focused on the dynamics of a particular species, we believe that our approach and findings may be useful in a much broader context. Synchronization of population fluctuations often occurs due to a combination of the effects of environmental stochasticity and dispersal. Discriminating between these two mechanisms is a considerable challenge, especially where they act on the same spatial scale. By studying the coupling between local populations with a time lag of one generation, we demonstrate a general method for separating them. Indeed, it is hard to see how spatially-correlated stochastic fluctuations in weather conditions (as required by the Moran theorem) can possibly deliver a time-lagged coupling. The general message is therefore that within-generation synchrony can be attributed to the environment whilst that with a shift between generations, i.e. time-lagged, is due to dispersal.

References

Baars, M.A., and Van Dijk, T.S. (1984) Population dynamics of two carabid beetles at a Dutch heathland. I. Subpopulation fluctuations in relation to weather and dispersal. J. Anim. Ecol. 53, 375-88.

Bartlett, M.S. (1963) The spectral analysis of point processes. J. R. Statist. Soc. B 25(2), 264-296. Discussion on Professor Bartlett's paper, p. 294.

Benjamini, Y., and Hochberg, Y. (1995) Controlling the false discovery rate: a practical and powerful approach to multiple testing. J. R. Statisti. Soc. B 57(1), 289-300.

Blackshaw, R.P. (1983) The annual leatherjacket survey in Northern Irealnd, 1965-1982, and some factors affecting populations. Plant Path. 32, 345-349.

Blackshaw, R.P. and Coll, C. (1999) Economically important leatherjackets of grassland and cereals: biology, impact and control. Int. Pest. Man. Contr. 4, 143-160.

Blackshaw, R.P., and Petrovskii, S.V. (2007) Limitation and regulation of ecological populations: a meta-analysis of Tipula paludosa field data. Math. Model. Nat. Phenom. 2(4), 46-62.

Blackshaw, R.P., and Moore, J.P. (2012) Within-generation dynamics of leatherjackets (*Tipula paludosa* Meig.) J. Appl. Entomol. 136, 605613.

Compton, S.G. (2002) Sailing with the wind: dispersal by small flying insects. In *Dispersal ecology* (J.M. Bullock, R.E. Kenward, R.S. Hails, eds.), pp. 113-133. Blackwell, Oxford.

Earn, D.J.D., Levin, S.A., and Rohani, P. (2000) Coherence and conservation. Science 290, 1360-1364.

Gatehouse, A.G. (1997) Behavior and ecological genetics of wind-borne migration by insects. Annu. Rev. Entomol. 42, 475-502

Goldwyn, E.E. and Hastings, A. (2011) The roles of the Moran effect and dispersal in synchronizing oscillating populations. J. Theor. Biol. 289, 237-246.

Gotelli, N.J., and Ellison, A.M. (2004) A Primer of Ecological Statistics. Sinauer Associates, Sunderland.

Hanski, I., and Woiwod, I.P. (1993) Spatial synchrony in the dynamics of moth and aphid populations. J. Anim. Ecol. 62, 656-668.

Haydon D, Steen H. 1997. The effects of large and small-scale random events on the synchrony of metapopulation dynamics: a theoretical analysis. Proc. R. Soc. Lond. B 264, 1375-1381.

Holm, S. (1979). A simple sequentially rejective multiple test procedure. Scand. J. Statist. 6 (2), 60-65.

Hope, A. C. A. (1968). A simplified Monte Carlo significance test procedure. J. R. Statist. Soc. B 30 (3), 582-598.

Jackson, D. M. and R. L. Campbell (1975). Biology of the European cranefly, Tipula paludosa Meigaen, in western Washington (Tipulidae: Diptera). Technical Report 81, Washington State University.

Kaitala V, Ranta E, and Lundberg P. (2001) Self-organized dynamics in spatially structured populations. Proc. R. Soc. Lond. B 268, 1655-1660.

Kareiva, P. (1990) Population dynamics in spatially complex environments: theory and data. Phil. Trans. R. Soc. Lond. B 330, 175-190.

Kendall, B.E., Bjornstad, O.N., Bascompte, J., Keitt, T.H., and Fagan, W.F. (2000) Dispersal, environmental correlation, and spatial synchrony in population dynamics. Am. Nat. 155, 628-36.

Levin, S. (1976) Population dynamics models in heterogeneous environments. Ann. Rev. Ecol. Syst. 7, 287-310.

Liebhold, A., Koenig, W.D., and Bjornstad, O.N. (2004) Spatial synchrony in population dynamics. Annu. Rev. Ecol. Evol. Syst. 35, 467-490.

Lundberg, P., Ranta, E., Ripa, J., and Kaitala, V. (2000) Population variability in space and time. TREE 15, 460-464.

Lyles, D., Rosenstock, T.S., Hastings, A. and Brown, P.H. (2009) The Role of Large Environmental Noise in Masting: General Model and Example from Pistachio Trees. J. Theor. Biol. 259, 701-713.

Mayor, J.G., and Davies, M.H. (1976) A survey of leatherjacket populations in south-west England, 1963-1974. Plant Path. 25, 121-128.

Milne, A., Laughlin, R. and Coggins, R.E. (1965) The 1955 and 1959 population crashes of the leatherjacket, Tipula paludosa Meigen, in Northumberland. J. Anim. Ecol. 34, 529-534.

Moran, P.A.P. (1953a) The statistical analysis of the Canadian lynx cycle. I. Structure and prediction. Aust. J. Zool. 1, 163-173.

Moran, P.A.P. (1953b) The statistical analysis of the Canadian lynx cycle II. Synchronization and meterology. Austr. J. Zool. 1, 291-298.

Peltonen, M., Liebhold, A., Bjrnstad, O.N., and Williams, D.W. (2002) Variation in spatial synchrony among forest insect species: roles of regional stochasticity and dispersal. Ecology 83, 3120-3129.

Perneger, T.V. (1998) What's wrong with Bonferroni adjustments. Brit. Med. J. 316, 1236-1238.

Petrovskii, S.V., and Blackshaw, R. (2003). Behaviourally structured populations persist longer under harsh environmental conditions. Ecol. Lett. 6, 455-462.

Pickett, S., and Thompson, J. (1978) Patch dynamics and the design of nature reserves. Biol. Cons. 13, 27-37.

Pollard, E., Lakhani, K.H. and Rothery, P. (1987) The detection of density dependence from a series of annual censuses. Ecology 68, 2046-2055.

Post, E., and Forchhammer, M.C. (2002) Synchronization of animal population dynamics by large scale climate. Nature 420, 168-171.

Raimondo, S., Liebhold, A.M., Strazanac, J.S., and Butler, L. (2004) Population synchrony within and among Lepidoptera species in relation to weather, phylogeny, and larval phenology. Environ. Entomol. 29, 96-105.

Ranta, E., Kaitala, V., Lindstrom, K., Helle, E. (1997) Moran effect and synchrony in population dynamics. Oikos 78, 136-142.

Ripa, J. (2000) Analysing the Moran effect and dispersal: their significance and interaction in synchronous population dynamics. Oikos 89, 175-187.

Rohani, P., Earn,D., and Grenfell,B. (1999) Opposite patterns of synchrony in sympatric disease metapopulations. Science 286, 968-971.

Rosenstock, T.S., Hastings, A., Koenig, W.D., Lyles, D.J., and Brown, P.H. (2011) Testing Moran's theorem in an agroecosystem. Oikos 120, 1434-1440.

Royama, T. (1992) Analytical Population Dynamics, Chapman & Hall.

Sinclair, A.R.E., and Gosline, J.M. (1997) Solar activity and mammal cycles in the Northern hemisphere. Am. Nat. 149, 776-784.

Sutcliffe, O.L., Thomas, C.D., and Moss, D. (1996) Spatial synchrony and asynchrony in butterfly population dynamics. J. Anim. Ecol. 65, 85-95.

Sutcliffe, O.L., Thomas, C.D.,Yates, T.J., Greatorex-Davies, J.N. (1997) Correlated extinctions, colonizations and population fluctuations in a highly connected ringlet butterfly metapopulation. Oecologia 109, 235-241.

Vasseur, D.A., and Yodzis, P. (2004) The color of environmental noise. Ecology 85, 1146-1152.

Williams, D.W., and Liebhold, A.M. (1995) Influence of weather on the synchrony of gypsy moth (Lepidoptera: Lymantriidae) outbreaks in New England. Environ. Entomol. 24, 987-995.

Appendix: Statistical analysis of the population data

As described in the main text, in order to quantify the degree of synchronization between the populations of two fields (say, X and Y), we calculate the correlation coefficient of their respective residual time series, R^X and R^Y:

$$r_0(R^X, R^Y) = \frac{\sum_{i=2}^{n}(R_i^X - \mu_R^X)(R_i^Y - \mu_R^Y)}{\sqrt{(\sum_{i=2}^{n}(R_i^X - \mu_R^X)^2)\,(\sum_{i=2}^{n}(R_i^Y - \mu_R^Y)^2)}} \ ,$$

where R_i^X and R_i^Y are the residual population densities at year i in fields X and Y, respectively, and μ_R^X and μ_R^Y are the sample means of the two time series.

It is not immediately clear, however, what constitutes a statistically significant correlation coefficient. Since we work with time series of finite length, and the data are affected by stochastic factors, any given value of the correlation coefficient (5) may appear by chance. One must therefore distinguish between the cases when high absolute values of $r_0(R^X, R^Y)$ are superficial and the cases when these values are the result of actual synchronization. In order to do so, the following approach can be used. Suppose that the two time series used to calculate the correlation coefficient, r_0, are unsynchronised. Then, if one of these series is replaced with random residuals drawn from $\mathcal{LN}_R$ and the correlation coefficient is recalculated, the resulting distribution of correlation coefficients should be centred on r_0. Furthermore it is possible to estimate the probability of a higher absolute value of the correlation coefficient being obtained from a purely random time series. This approach constitutes a (two-tailed) Monte Carlo test as was originally described by Professor Barnard in (Bartlett 1963) and later refined by Hope (1968).

In particular, we start from the assumption (or null hypothesis) that two populations are not synchronised, that is that any correlation between them occurs by chance. The probability of obtaining the observed correlation coefficient given this assumption, called the p-value, is calculated as described below. If this probability falls below a certain significance level, denoted α, then our initial assumption is rejected and instead the populations are considered synchronised. Hence, for a single test, the significance level is the probability of incorrectly rejecting the null hypothesis, i.e. a false positive or Type I error; e.g. see Gotelli and Ellison (2004).

Monte Carlo test. Random variates from the distribution $\mathcal{LN}_{\mathcal{R}}$ were used to construct time series of residuals, R^*. A correlation coefficient, $\bar{r}_0$, for each (R^X, R^*) pair was calculated and compared with r_0, the value obtained for (R^X, R^Y). The number of pairs

for which $\bar{r}_0 > r_0$ was then divided by the total number of trials to determine the estimated p-value of r_0. An initial run of 500 permutations were used to obtain a crude p-value, p_c. If $p_c > 0.2$ then the pair were considered not significantly correlated without further calculation. If $p_c < 0.2$ a further run of 50000 permutations were used to obtain a refined p-value, p_r.

Note that the number of random permutations used in the refinement run are high relative to those proposed in (Bartlett 1963) and (Hope 1968). It was determined heuristically that this number was required to ensure consistent results at the lowest significance level used $\alpha = 0.05$. The initial crude assessment allows computational run time to be reduced if the majority of time series assessed are not strongly correlated.

Multiple comparisons and significance level. In assessing the synchronization of each distinct pair of populations included in the study a large number of statistical tests must be carried out. It is intuitively clear that undertaking more tests increases the number of false positives obtained. In order to maintain the desired significance level over the entire family of inferences undertaken it is necessary to account for this in some way without excessively compromising the power of the test (Perneger 1998). This is achieved by defining an acceptable false positive rate (Benjamini and Hochberg 1995).

Note first that we have a finite set of N distinct events, $\{A_i : 1 \leq i \leq N\}$, representing each instance where the null hypothesis might be falsely rejected. The union of these events corresponds to obtaining at least one false positive. A limit on the probability of this union is given by Boole's inequality:

$$P(\cup_i A_i) \leq \sum_i P(A_i), \tag{9}$$

in terms of the probability of each individual false positive.

Thus to control the false positive rate we first place the correlation values obtained in ascending order according to their p-value. A given null hypothesis is then rejected only if the sum of its p-value with those of all tests ranked below it is less than the desired family significance level. Once the cumulative p-value exceeds this level all remaining null hypotheses are accepted, that is all remaining populations are considered to be unsynchronised. Thus the probability of at least one false positive is restricted by Boole's inequality to less than the family significance level.